

# Slender high strength steel column laterally supported by glass panes

D. Dierks, E.M.P. Huveners  
Volantis, Venlo, the Netherlands

H.H. Snijder, R.C. Spoorenberg  
Eindhoven University of Technology, Eindhoven, the Netherlands

**Structural steel is a material that allows for slender columns. However, slender steel columns usually have a low load bearing resistance due to flexural buckling. It is possible to suppress flexural column buckling by adding glass panes. Thus, use can be made of the steel section's squash load reducing the amount of steel involved and obtaining a highly transparent glass-steel column. In this paper, a new type of slender transparent glass-steel column is proposed, consisting of a high strength steel bar supported in lateral direction by glass panes. Its feasibility is shown experimentally and numerically. It is also shown that the design has sufficient redundancy to allow for the loss of supporting glass panes without a reduction of the load bearing capacity. The key design feature of this glass-steel column is the way the glass panes are connected to the steel bar, namely by sliding steel sleeves to avoid direct stresses to occur in the glass panes due to axial column deformation.**

*Keywords: High strength steel, column, glass panes, flexural buckling, redundancy, epoxy adhesive bonded joint, finite element analyses, experiments*

## 1 Introduction

Transparency and slenderness are getting more and more important in modern architecture and are also very relevant for columns.

Glass is a material that allows for transparency. In general, glass is a brittle material and therefore special attention has to be paid to structural safety. Several research projects have been carried out to investigate glass columns. Overend [1] investigated cruciform and tubular glass columns. Nieuwenhuijzen [2] investigated laminated tubular glass columns.

Both research projects concluded that the end connections are essential elements for proper load introduction. Luible [3] investigated stability effects on small slender glass elements.

Structural steel allows for slender columns but then loss of stability through flexural buckling is the dominant failure mode reducing the load bearing resistance. If flexural buckling is suppressed effectively, the full squash load of the steel column can be achieved.

In view of the architectural qualities glass can offer and the good performance that structural steel has, a glass-steel column where glass panes suppress the occurrence of flexural buckling can be regarded as an excellent structural composite element. A glass-steel column must be designed such that flexural buckling of the steel column is suppressed by laterally supporting glass panes. Roebroek [4] and [5] investigated a slender steel column in normal grade steel, laterally supported by a locally connected glass pane. He showed that it is possible to support a full scale slender steel column laterally by one locally connected glass pane thereby remarkably increasing its load bearing resistance.

If flexural buckling of steel columns can be suppressed effectively and the full yield stress can be utilized, it makes sense to use high-strength steel to further reduce the use of material. The present study [6] focussed on the design of a high strength steel bar laterally supported glass panes connected by sliding glass-steel sleeve connections to avoid direct stresses to occur in the glass panes. The structural response of the proposed glass-steel column is examined by means of experiments and finite element analyses. Special attention is paid to the loss of one or more glass panes, reducing the number of panes supporting the steel bar, showing the glass-steel column to have sufficient redundancy.

## **2 Design of the glass-steel column**

By using high strength steel for the glass-steel column, less steel was needed to achieve a similar squash load as for the normal steel grade S235. However, less and higher strength steel results in a more slender column with flexural buckling becoming even more predominant. To utilize the full yield stress of the high strength steel, glass panes were added as lateral supports to suppress flexural buckling. Eurocode 3 [7] was used as preliminary design tool and sensitivity analyses using finite element software were then used to further design the glass-steel column.

The design of the glass-steel column is shown in the figures 1 and 2. The glass-steel column consists of a high strength steel bar supported by glass panes which are connected through sliding sleeves to the steel bar. The glass panes are slightly shorter than the height of the steel bar to keep them free from roof and floor. Heat strengthened float glass resists a higher maximum principal stress (i.e. tension) than anneal float glass and offers more residual capacity than fully tempered float glass [8]. Therefore, the four supporting glass panes in crucifix arrangement are made of heat strengthened float glass. Using four glass panes, two for each direction, allows losing one glass pane per direction without reduction of bearing resistance thus giving the design redundancy. Only at the lower support, the sleeve is fixed to the bar. All other sleeves are sliding vertically to avoid direct stresses to occur in the glass panes caused by axial column deformation. Adhesively bonded stainless steel strips connect the glass panes to the lips welded to the sleeves.

### 2.1 Support spacing

The steel bar used is a plain Dywidag bar with steel grade St 950/1050 [9]. Threaded ends on the plain bar are used for realizing the end supports. The diameter is 32 mm and the total height is 3600 mm, i.e. one story high. Although the steel grade of the bar is greater than the highest steel grade S700 covered by Eurocode 3, Eurocode 3 is used for designing the glass-steel column. This is justified by several studies showing that high strength steel performs better with respect to flexural buckling of columns than normal grade steel or at least not worse [10]. The reason for this better behaviour is a smaller influence of residual stresses.

The spacing between the lateral supports, i.e. the spacing between the sleeves, is determined using the flexural buckling design rule according to Eurocode 3 assuming the steel bar to buckle locally between the lateral supports (sleeves):

$$\frac{N_{Ed}}{N_{b,Rd}} \leq 1.0 \quad (1)$$

where:

$N_{Ed}$  is the compressive design load [kN]

$N_{b,Rd}$  is the buckling resistance [kN] governed by the squash load (i.e.  $804 \text{ mm}^2 \times 950 \text{ N/mm}^2 \times 10^{-3} = 764 \text{ kN}$ ) multiplied by a reduction factor  $\chi$  to include the effect of flexural buckling

A spacing between lateral supports  $L_{sup} = 150$  mm is adopted. According to Eurocode 3 this leads to a reduction factor  $\chi = 0.936$ , resulting in  $N_{b,Rd} = 715$  kN.

## 2.2 Glass-steel connection

Two-compound epoxy adhesive 3M Scotch-Welt 9323 B/A [11] as used by Roebroek [4] and examined by Huveners [12], is used to connect the glass panes to stainless steel strips. The adhesive bonded joint has an area of approximately  $30 \times 35$  mm<sup>2</sup> and a nominal thickness of 0.5 mm which is achieved by acrylate spacers. The strips are bolted to lips welded to the sleeves that support the steel bar locally. Each mid sleeve holds two glass panes placed perpendicularly (figure 1, middle). The top and bottom sleeve hold all four glass panes placed perpendicularly (figure 1, left and right). Each mid sleeve rotates 180° with respect to the previous one (figure 2, left).

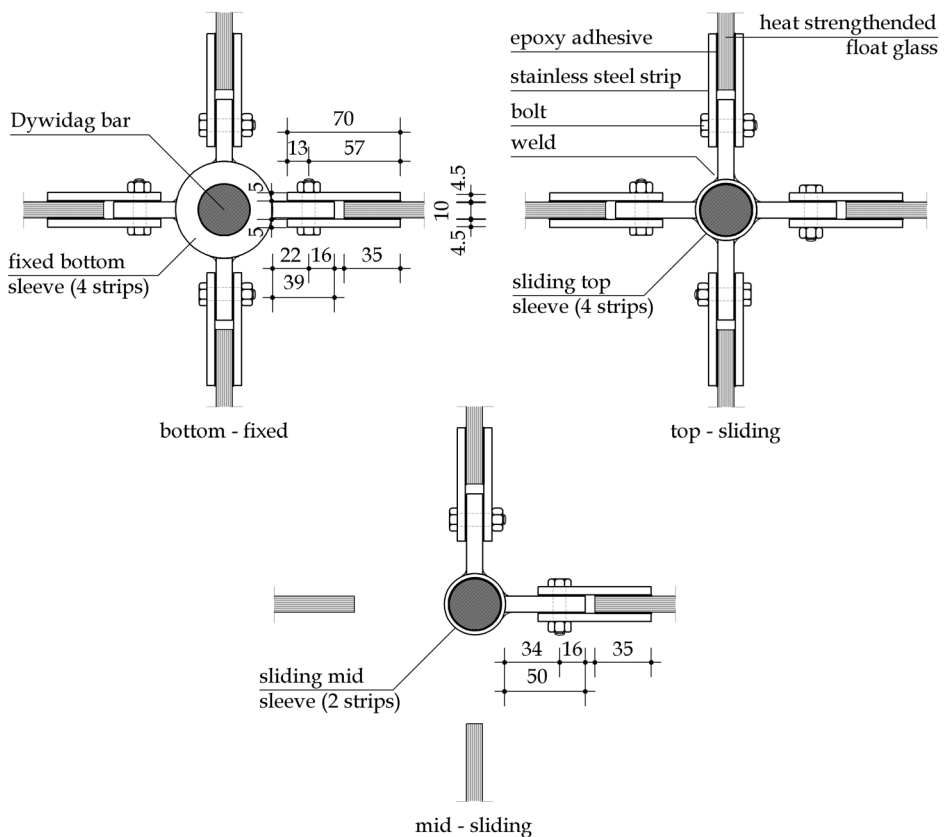


Figure 1: Cross-sections of the sleeves with two or four glass panes attached

### 2.3 Steel bar end supports

To realize the steel bar's end supports, a Dywidag coupling connector was used at the threaded ends (figure 1 and 2, left). This connector is 110 mm long and has a diameter of 60 mm.

### 2.4 Finite element analyses for fine tuning

To fine tune the preliminary glass-steel column design, finite element (FE) simulations are carried out. Section 4 discusses FE simulations in more detail. Material behaviour of the high strength steel is needed as input data for the analyses. These data are obtained by small scale tests performed on coupons taken from a spare steel bar (section 3.1) and simplified by a bi-linear stress-strain curve. The small scale tests revealed a lower yield stress under compression which lowered the squash load from 764 kN to 523 kN. Linear buckling analyses were used for fine tuning the preliminary design based on Eurocode 3. Variations were made in the support spacing  $L_{sup}$ , the unsupported end lengths  $L_{end}$ , the connector length  $L_{con}$  and the glass pane width  $w_{glass}$ , presented in figure 2. The total height  $L_{tot}$  and glass pane thickness were kept constant at 3600 mm and 20 mm

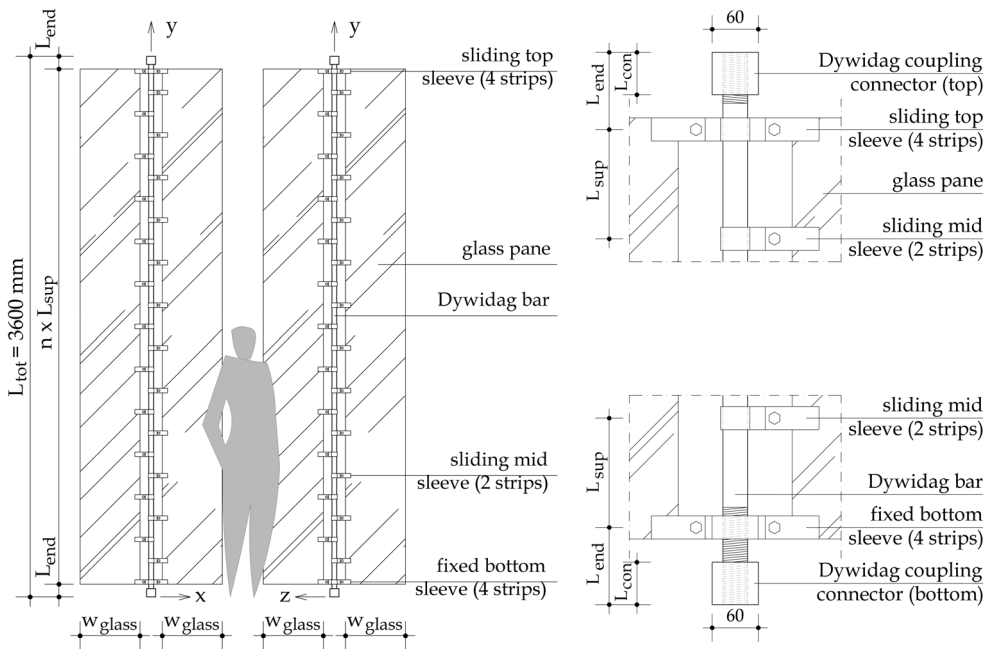


Figure 2: Preliminary glass-steel column design

respectively. In each series of analyses one or a set of related parameters were varied. To examine the influence of the boundary conditions on the critical load, pin-ended or clamp-ended supports were used.

The most important feature is the buckling mode of the glass-steel column. The anticipated flexural buckling mode is buckling locally between the lateral supports (i.e. the sleeves) which only occurs for the clamp-ended glass-steel column. The pin-ended glass-steel column buckles in a global mode (table 1).

Table 1: Linear buckling analyses mode shapes (steel bar only) and critical loads

	Pin-ended glass-steel column	Clamp-ended glass-steel column
$L_{sup} = 142 \text{ mm}$		
$L_{end} = 100 \text{ mm}$		
$L_{con} = 55 \text{ mm}$		
$w_{glass} = 600 \text{ mm}$		
critical load	1190 kN	4550 kN

Geometrical and material non-linear imperfection analyses (GMNIA) with the geometrical dimensions presented in table 1 are carried out to examine principal stresses in the glass panes. Four scenarios are simulated:

- four glass panes;
- three glass panes;
- two glass panes placed perpendicularly;
- two glass panes placed parallel.

The first Euler buckling mode is used as geometrical imperfection shape in the x-y plane only, i.e. a sinusoidal imperfection. The maximum amplitude of this imperfection is  $e^* = l_{tot} / 1000 = 3.6 \text{ mm}$ .

Table 2 presents the ultimate loads  $N_{ult}$  and the maximum principal glass stresses  $\sigma_1$  (tensile). Only the clamp-ended glass-steel column is able to reach the steel bar's squash load of 523 kN. Even with two glass panes placed perpendicularly as lateral supports, the squash load is reached. Therefore, the clamp-ended glass-steel column shows more

redundancy than the pin-ended glass-steel column. The reason for the ultimate loads in table 2 being greater than found in the small scale tests is loading beyond the yield stress. Finally, it was decided to design the glass-steel column with clamped ends.

### 3 Experimental programme

Since experiments are often expensive and time consuming, it is the intention to perform a limited number of tests to validate a FE model. The experimental programme consists of two types of tests: small scale tests and full scale tests.

#### 3.1 Small scale tests

Prior to the full scale tests, small scale tests were carried out. The goal of these small scale tests was to obtain material properties to be used as input data for the FE simulations. All small scale test specimens were taken from the same steel bar. Tensile, compression and buckling tests were carried out. NEN-EN-10002-1 [13] was adopted for the tensile tests. Ziemian [14] was used for the compression and buckling tests.

A 250 kN Schenck servo-controlled screw-driven testing machine with hydraulic end grips was used for the tensile tests. Due to the limitation in load capacity, the specimen cross-section was reduced to a diameter of 16 mm. Care has been taken not to overheat the specimens.

The compression and buckling tests were carried out with a displacement controlled 2.5 MN actuator. To ensure a smooth surface for adhesively bonded strain gauges, the diameter of each specimen was reduced to 30 mm. Again, care has been taken not to

Table 2: GMNIA results

Steel bar supported by:	Glass-steel column			
	Pin-ended		Clamp-ended	
	$N_{ult}$ [kN]	$\sigma_1$ [N/mm <sup>2</sup> ]	$N_{ult}$ [kN]	$\sigma_1$ [N/mm <sup>2</sup> ]
four glass panes	470	7.2	591	16.1
three glass panes	470	7.5	551	25.5
two glass panes placed perpendicularly	281	6.2	530	8.4
two glass panes placed parallel	11	21.1	42	38.5

overheat the specimens. The length of the specimens was 50 mm for the compression tests and 300 mm for the buckling tests. The buckling test specimens were placed between spherical supports to trigger buckling. An impression of the test setups is presented in figure 3.

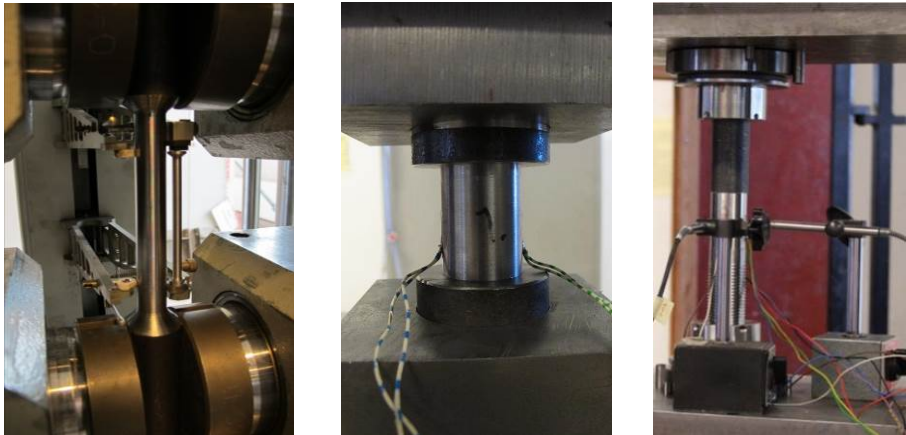


Figure 3: Small scale test: tensile test (left), compression (middle), buckling (right)

The engineering stress-strain curves of the small scale tests are presented in figure 4. The tensile and buckling tests showed a clear yield plateau at  $975 \text{ N/mm}^2$  and  $650 \text{ N/mm}^2$  respectively. The compression tests showed gradual yielding between  $550 \text{ N/mm}^2$  and  $625 \text{ N/mm}^2$ . The small scale tests revealed different yield stresses under compression and tension. The yield stress in compression was significantly lower than the yield stress in tension:  $650 \text{ N/mm}^2$  and  $975 \text{ N/mm}^2$  respectively. This was caused by the production process of the Dywidag bar and can be attributed to the Bauschinger effect.

Although the small scale buckling tests were setup to trigger buckling, buckling did not occur in the tests. Accidentally, small scale buckling tests were very good representations for small scale compression tests (figure 4, right). Therefore the material properties found in the small scale buckling tests were used as input data for the FE simulations.

### 3.2 Full scale tests

The full scale test programme consisted of one glass-steel column which was tested four times, changing the number of glass panes for lateral support in each test. Single panes of heat strengthened float glass with a height of 3431 mm were used. The diameter of the steel

bar was measured over the entire height and averaged to 32.3 mm which resulted in an average cross-sectional area of 819 mm<sup>2</sup>. A schematic overview of the full scale tests is presented in table 3.

The steel bar was placed in a rigid steel frame and then the glass-steel column was assembled (figure 7). After assembly the geometrical imperfections of the steel bar were measured by means of a theodolite and presented in the figures 5 and 6.

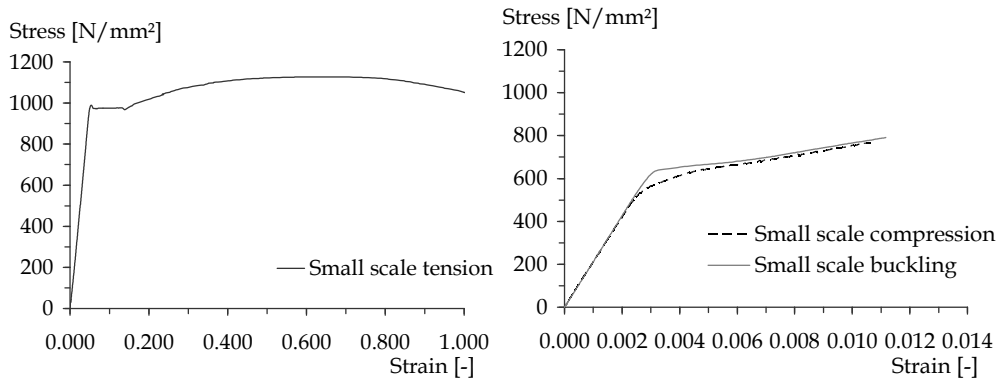


Figure 4: Engineering stress-strain curves of the small scale tests

Table 3: Overview of the full scale tests

	Test 1	Test 2	Test 3	Test 4
number of glass panes	4	3	3 - 2	0
$L_{tot}$	3600 mm	3600 mm	3600 mm	3600 mm
$L_{sup}$	142 mm	142 mm	142 - 284 mm	-
$L_{end}$	100 mm	100 mm	100 mm	-
$L_{con}$	55 mm	55 mm	55 mm	55 mm
$w_{glass}$	400 mm	400 mm	400 mm	-
$w_{glass}$	10 mm	10 mm	10 mm	-

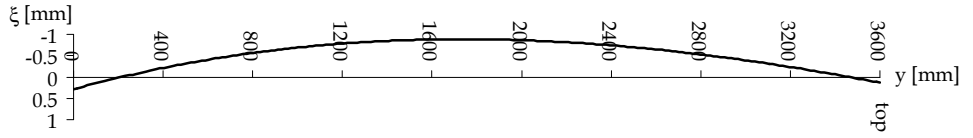


Figure 5: Geometrical imperfections of the steel bar in the  $\xi$ - $y$  plane (also see figure 7)

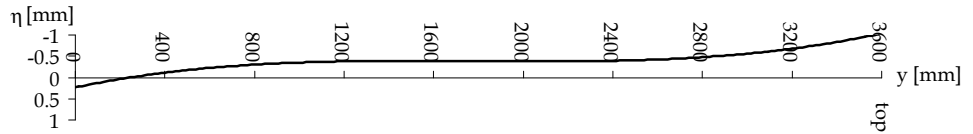


Figure 6: Geometrical imperfections of the steel bar in the  $\eta$ - $y$  plane (also see figure 7)

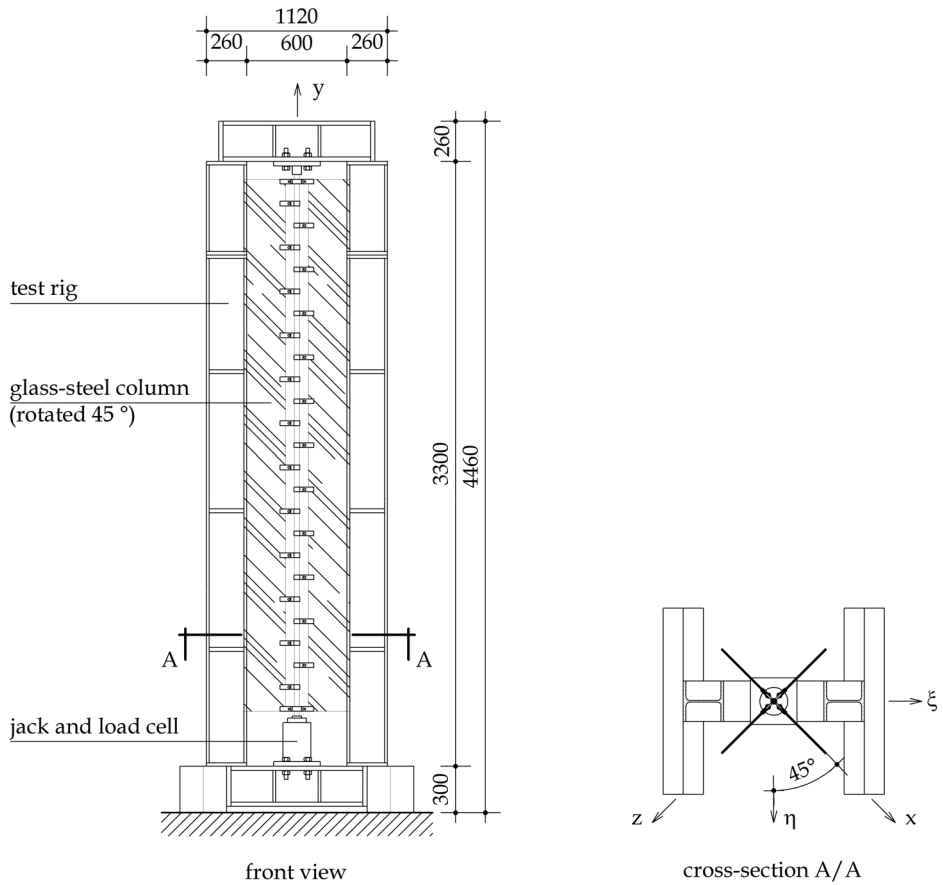


Figure 7: Full scale glass-steel column positioned in test frame



Figure 8: Full scale glass-steel column positioned in test frame, top sleeve and bottom sleeve

In the FE analyses discussed in section 2.4 the maximum (tensile) principal glass pane stresses were found at the top and bottom glass-steel connections. Therefore strain gauge rosettes were placed at these locations to measure the strains on the glass during the tests.

To monitor the steel bar's strain, two times four electrical strain gauges were applied around the bar's circumference at the bottom and at mid height. The glass-steel column's displacement was measured at the point of load introduction at the bottom sleeve (figure 8, right). Sliding of the sleeves was measured at the top sleeve (figure 8, left).

### 3.2.1 Test 1, lateral support by four glass panes

Loading was applied manually by an upward displacement of approximately 0.2 mm/min at the bottom of the steel bar. The loading was stopped at 300 kN and 400 kN for approximately five minutes to allow settlements to occur. At 525 kN the experiment was terminated to be able to reuse the glass-steel column in subsequent tests.

Figure 9 (left) presents the load-displacement curve of the top (sliding) and bottom (fixed) sleeve in test 1. The bottom sleeve shows an initial displacement of 0.7 mm. Up to approximately 500 kN the load-displacement curve was almost linear, beyond 500 kN the

curve started to deflect more (i.e. elastic-plastic range). At 525 kN the stress in the steel bar is 641 N/mm<sup>2</sup> which is similar to the yield stress found in the small scale buckling tests: the steel bar almost yields.

At 500 kN the top sleeve displacement was 9.9 mm which is similar to the elastic displacement of 10.3 mm found with Hooke's Law. The bottom sleeve displacement was 13.8 mm. The bottom thread deformation in the Dywidag connector was 1.2 mm as is shown in figure 9 (right). There are two of these connections, resulting in a total thread deformation of 2.4 mm. Adding this thread deformation to the initial displacement of 0.7 mm and subtracting the result from the measured 13.8 mm results in a bottom sleeve displacement of 10.7 mm which is 0.4 mm greater than according to Hooke's law. This difference can be attributed to a locally reduced diameter at the bar's threaded end parts and settlements in the test setup.

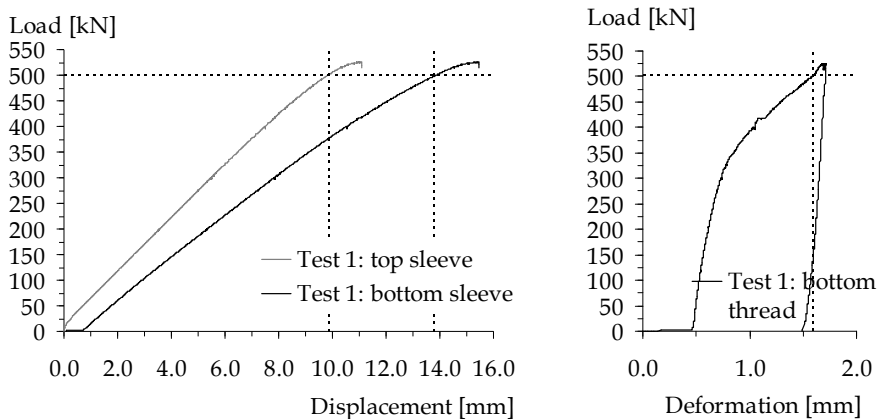


Figure 9: Load-displacement curves of top and bottom sleeve (left) and bottom thread (right)

### 3.2.2 Test 2, lateral support by three glass panes

The loading procedure of test 2 was identical to that of test 1. The load increased linearly up to 499 kN at which level the second highest sliding sleeve seized resulting in a locally cracked glass pane at the top glass-steel connection (figure 10). After cracking, the load dropped to 480 kN and the test was terminated. Figure 11 (left) presents the load-displacement curve of the top (sliding) and bottom (fixed) sleeve in test 2. The bottom sleeve shows an initial displacement of 0.4 mm. The curve of the top sleeve clearly shows



Figure 10: Seized second highest sliding sleeve and locally cracked glass pane

seizing. An increased principal stress in the glass panes was not observed.

At 499 kN the bottom sleeve deformed 11.8 mm, which is 1.5 mm greater than according to Hooke's law. The thread deformation in the connector at both column ends was  $2 \times 0.2$  mm (figure 11, right). Adding this deformation to the initial displacement and subtracting the result from the measured value of 11.8 mm results in a bottom sleeve deformation of 11.0 mm. This is 0.7 mm greater than according to Hooke's law and can be explained by the reasons given for test 1.

### 3.2.3 Test 3, lateral support by three and finally two glass panes

The loading procedure of test 3 was identical to that of the previous tests. The load increased linearly up to 314 kN, at which level several glass connections of one glass pane unexpectedly failed locally (figure 12). Residual lateral support of the locally failed glass

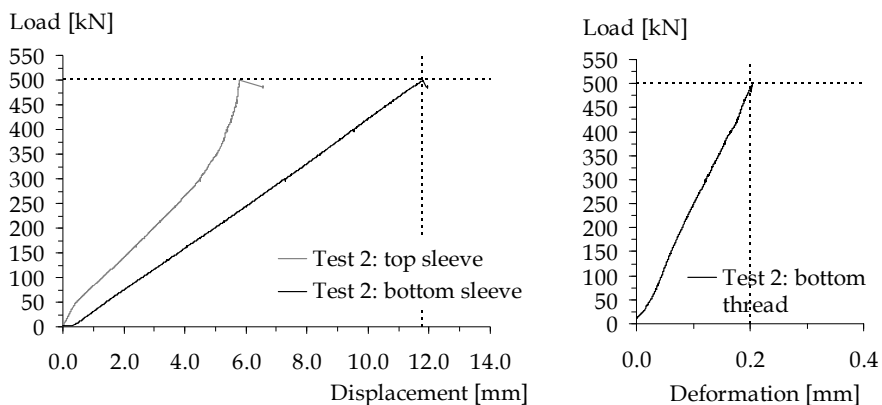


Figure 11: Load-displacement curves of top and bottom sleeve (left) and bottom thread (right)



Figure 12: Locally failed glass pane in test 3

panes was assumed to be negligible. Loading was continued up to 520 kN.

Figure 13 (left) presents the load-displacement curve of the top (sliding) and bottom (fixed) sleeve in test 3. As in test 2, the bottom sleeve shows an initial displacement of 0.4 mm. At 314 kN, failure of one glass pane, the curve shifts 0.3 mm. The curve of the top sleeve clearly shows seizing over the entire load path.

At 500 kN the bottom sleeve deformed 11.8 mm, which is 1.5 mm greater than according to Hooke's law. The thread deformation in the connector at both column ends was  $2 \times 0.14$  mm (figure 13, right). Adding this deformation to the initial displacement and subtracting the result from the measured value 11.8 mm results in a bottom sleeve deformation of

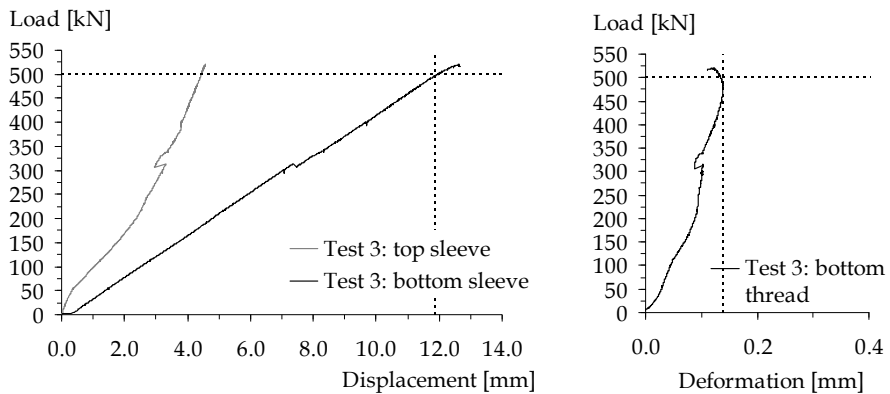


Figure 13: Load-displacement curves of top and bottom sleeve (left) and bottom thread (right)

11.1 mm. This is 0.8 mm greater than according to Hooke's law and can be explained by the reasons given previously for test 1.

### 3.2.4 Test 4, single steel bar

Loading was applied manually by an upward displacement of approximately 0.002 mm/min until buckling occurred.

Figure 14 shows the load-deflection curve at bar mid height. Between 20 and 30 kN the steel bar starts to buckle. Close to the Euler buckling load of 35 kN of a clamp-ended column the steel bar failed.

## 4 Finite element simulations

A validated FE model offers the possibility to investigate the structural response of glass-steel columns outside the scope of the experimental programme. In this paper, the FE model has been validated only on the load-displacement curves of the experiments which are discussed in chapter 3. In future research projects in the field of glass-steel columns this FE model can be adapted and improve for use in a parameter study. FE code ANSYS V11.0 [15] has been employed to simulate the structural response of the tested glass-steel columns performing GMNIA. True geometrical imperfections of the steel bar (section 3.2) were adopted. As it is impossible to include all geometrical and physical properties in a FE model, simplifications have to be made. The most important simplifications can be summarized as follows:

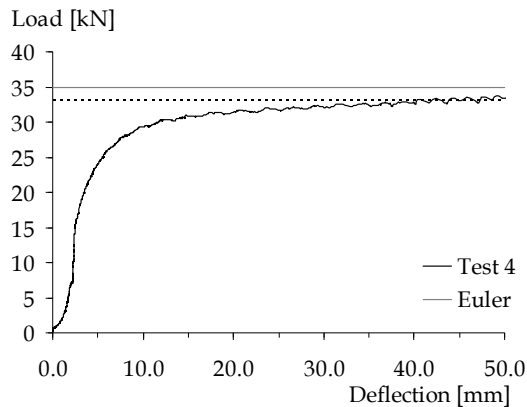


Figure 14: Load-deflection curve

- sliding sleeves were modelled fully, ignoring any friction effects;
- thread deformation of the top and bottom Dywidag connector is modelled by a linear spring having a fixed stiffness value;
- perfectly isotropic material behaviour for all materials;
- perfectly round steel bar (i.e. no cross-sectional deviation from ideal geometry other than the diameter);
- geometrical imperfections of the glass panes were neglected;
- crack behaviour of glass is not modelled.

Geometrical dimensions from table 3 were used in the FE analyses. An overview of the FE model is shown in figure 15. The main differences between the simulations discussed in this section and those discussed in section 2.4 are a multi-linear material behaviour of the steel bar, a spring element for the Dywidag connector and true geometrical imperfections as discussed in section 3.2.

#### 4.1 *Description of the finite element model*

##### 4.1.1 *Elements and material laws*

Element type Beam188 was used to model the steel bar. When dealing with GMNIA the engineering stress-strain curve is not adequate. Instead a true stress-strain curve is needed. The small scale buckling engineering stress-strain curve was modified into a true stress - logarithmic strain curve using the following equations:

$$\sigma_{\text{true}} = \sigma_{\text{engineering}} (1 + \epsilon_{\text{engineering}}) \quad (2)$$

$$\epsilon_{\text{ln}} = \ln(1 + \epsilon_{\text{engineering}}) \quad (3)$$

A multi-linear material model, using the multi-linear isotropic hardening option, was used to approximate the true stress-strain curve (figure 16). The Young's modulus of 215000 N/mm<sup>2</sup> follows from the true stress-strain curve.

Element type Shell181 was adopted to model the glass panes. Direct failure of the glass panes was not simulated. Failure was manually governed in the post-processor by checking the principal stresses. It was assumed that the glass pane fails if the principal stress reached 70 N/mm<sup>2</sup>, i.e. the nominal tension strength of heat strengthened float glass. A linear elastic material model with a Young's modulus of 70000 N/mm<sup>2</sup> and Poisson ratio

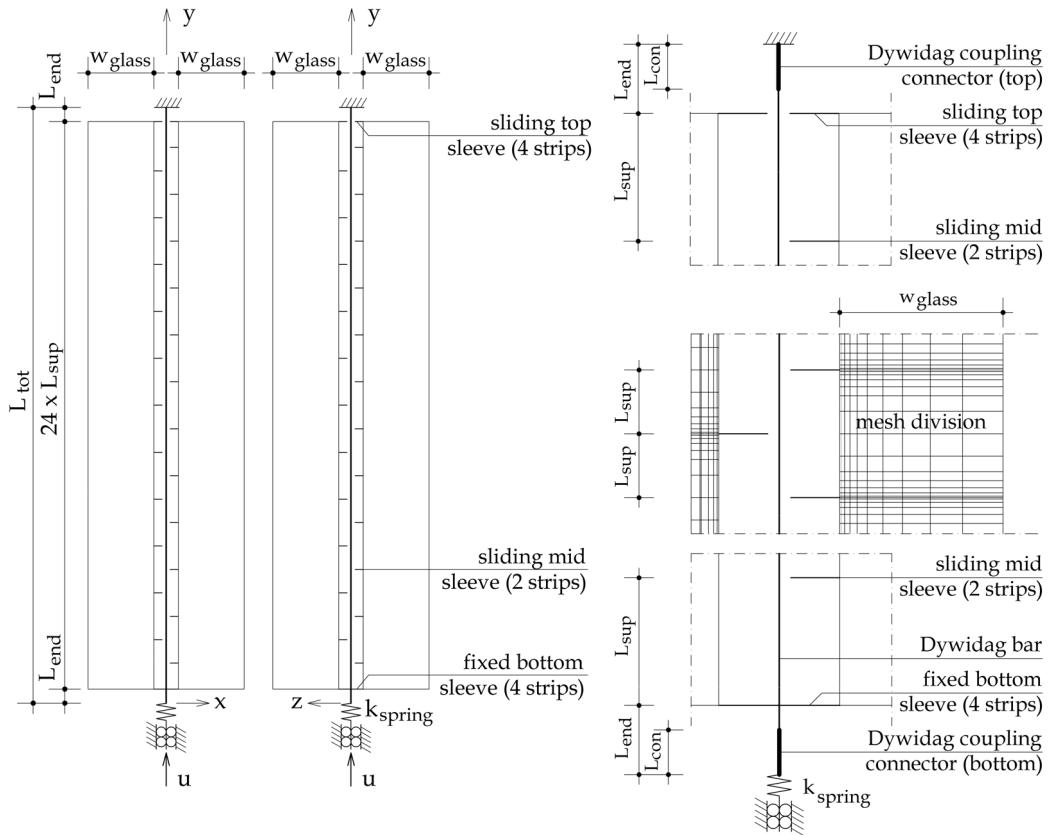


Figure 15: Overview of the finite element model geometry

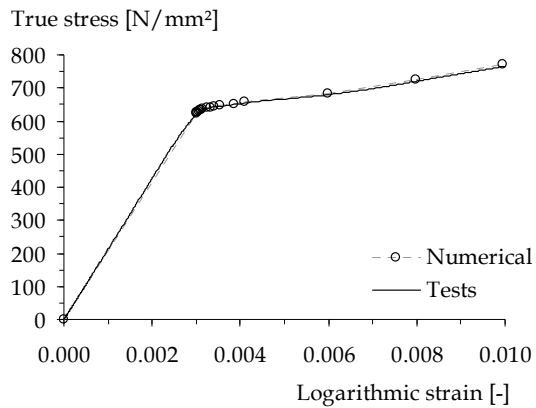


Figure 16: True stress-strain curve (numerical)

of 0.23 [-] was used for the glass panes.

Mesh refinement analyses have been performed using GMNIA. For element type Shell181 it was found that a mesh refinement towards the glass-strip connection (middle right picture in figure 15) gave the best results in ultimate load and principal stresses at moderate computational time.

#### 4.1.2 *Boundary conditions*

All sleeves, except the bottom one, were idealized as sliding connections. Sliding was modelled by a pair of coupled nodes. The longitudinal thread deformations in the top and bottom end Dywidag connectors were modelled together by one spring element of type Combin14 at the bottom. The stiffness was determined using the load-deformation curve of figure 9 (right). This resulted in the following spring stiffness:

$$k_{\text{spring}} = 2 \times (525000 \text{ N} / 1.7 \text{ mm}) = 618 \times 10^3 \text{ N/mm}.$$

Full scale test 4 showed a similar buckling load as the Euler clamp-ended column. Therefore the end supports were modelled as true clamped supports.

#### 4.1.3 *Loading*

The glass-steel column was loaded by an upwards displacement  $u$  at the bottom of the spring element. The applied displacement in each simulation was identical to the applied displacement in the full scale tests 1, 2 and 3. The total displacement was divided into four displacement steps. Within each displacement step a solution was obtained by applying the displacement incrementally in fifty sub steps.

### 4.2 *Validation of the finite element model*

#### 4.2.1 *Simulation of test 1*

At a displacement of 14.3 mm, which was the bottom sleeve displacement of 15.0 mm minus the initial displacement of 0.7 mm in test 1 at 525 kN, the finite element load was 526 kN. The simulation of test 1 was able to replicate the load-displacement curve as found in the test very well (figure 17).

#### 4.2.2 *Simulation of test 2*

At a displacement of 11.4 mm, which was the bottom sleeve displacement of 11.8 mm minus the initial displacement of 0.4 mm in test 1 at 499 kN, the finite element load was

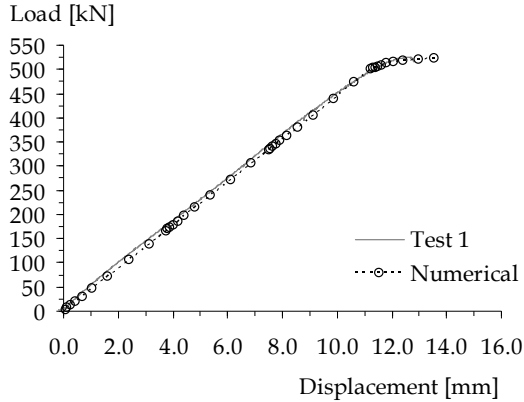


Figure 17: Load-displacement curves of test 1 and simulation

495 kN. The simulation of test 2 was able to replicate the load-displacement curve as found in the test also very well (figure 18).

#### 4.2.3 Simulation of test 3

The locally failed glass pane in test 3 was deactivated at 314 kN in the simulation. After that, loading was continued with the support of the two remaining glass panes.

At a displacement of 12.2 mm, which was the bottom sleeve displacement of 12.6 mm minus the initial displacement of 0.4 mm in test 3 at 520 kN, the finite element load was 519 kN. The simulation of test 3 was able to replicate the load-displacement curve as found in the test very well (figure 19).

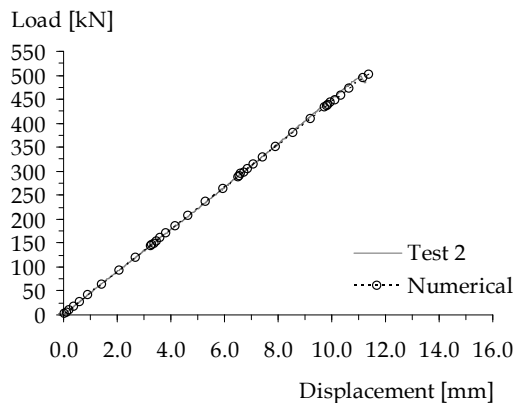


Figure 18: Load-displacement curves of test 2 and simulation

## 5 Discussion

The present glass-steel column uses high strength steel and sliding glass-steel sleeve connections. The load bearing resistance of the clamp-ended glass-steel column increased from 33 kN to 525 kN by adding four glass panes as lateral support to the steel bar. The design has sufficient redundancy as was confirmed by the full scale tests. Especially test 3 showed redundancy since the steel bar was laterally supported by two glass panes placed perpendicularly after failure of one glass pane and still a load of 520 kN was reached. The sudden local glass pane failure at a load of 314 kN in test 3 could not be explained.

In test 2 the second highest sliding sleeve seized on the threaded part of the steel bar inducing glass pane failure. Sliding sleeves on threaded parts are therefore to be avoided in the design.

An overview of experimental and simulated loads is presented in table 4. The FE model was able to replicate the load-displacement curves of the tests with good accuracy. The differences between experimental and numerical maximum loads were only 0.8%.

In table 5 the present glass-steel column is compared with an earlier version of a glass-steel column [4] and [5] and traditional pin-ended I shaped steel columns in normal steel grade S235 being 3600 mm long. Eurocode 3 has been adopted to determine the buckling resistances  $N_{b,Rd}$  with respect to the columns' weakest axes. The present glass-steel column is able to resist about as much load as traditional sections but it is far more transparent.

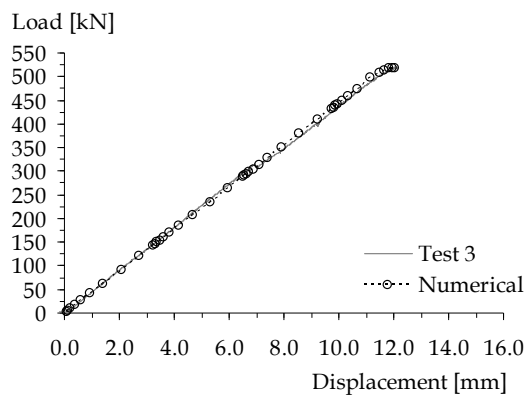


Figure 19: Load-displacement curves of test 3 and simulation

## 6 Conclusions

It was possible to laterally support a high strength steel bar by glass panes and utilize the steel bar's squash load in tests 1 and 3. Although the squash load was not reached in test 2 because the second highest sleeve seized on the bar's thread, it is most likely that the squash load could be reached if sliding of the second highest sleeve was assured. From test 3 it can be concluded that the steel bar required little lateral support to fully suppress flexural buckling. This test also showed that the design has redundancy.

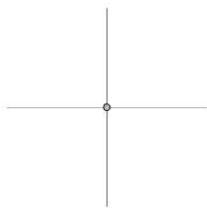
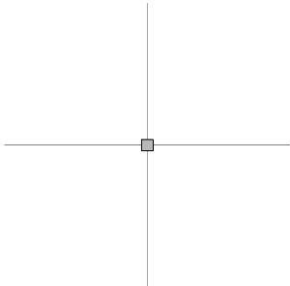
The restraining effect (i.e. suppressing buckling) of the glass panes was observed both in experiments and simulations. It was shown that a very slender high strength steel bar can be used as a column if restrained adequately by glass panes. The feasibility of this design was demonstrated.

It was possible to simulate the tested glass-steel column with sufficient accuracy. However more tests need to be carried out to fine tune the present FE model of the glass-steel

Table 4: Overview of the experimental and simulated loads

Test setup	Experiment	Simulation	Differences
1	525 kN	526 kN	0.2 %
2	499 kN	495 kN	0.8 %
3	520 kN	519 kN	0.2 %
4	35 kN	35 kN	0.0 %

Table 5: Overview of load bearing capacities

<i>Present design</i>	<i>Roebroek's design [4, 5]</i>	<i>IPE 270</i>	<i>HEA160</i>
			
(Clamp-ended)	(Pin-ended)	(Pin-ended)	(Pin-ended)
Squash load = 525 kN	Squash load = 699 kN	$N_{b,Rd} = 486$ kN	$N_{b,Rd} = 573$ kN

column. Then it makes sense to carry out a parametric study to investigate the structural response of glass-steel columns outside the scope of the experimental programme.

Due to the production process of the Dywidag steel bar the yield stress in compression was approximately 30% lower than in tension, resulting in a reduction in load bearing resistance even when sufficient lateral support was present.

In order to avoid direct stresses to occur in the glass panes, sliding sleeves were used in the design to connect the glass panes to the steel bar and these were shown to be effective.

The design of the glass-steel column consisting of a steel bar laterally supported by glass panes through sliding sleeves has sufficient redundancy: two out of four glass panes placed perpendicularly can fail without significantly affecting the load bearing resistance of the glass-steel column.

## **7 Recommendations**

The present glass-steel column design possessed some drawbacks. For future research projects in the field of glass-steel columns, the following recommendations are made:

1. Concerning the experiments it is recommended to increase the number of glass-steel column specimens. Experimental observations in this paper were based on a single glass-steel column only;
2. Only one glass pane width was used to laterally support the present glass-steel column. Other glass pane widths should be used to investigate the effect of the glass pane width on suppressing flexural buckling;
3. The Dywidag steel bar showed a lower yield stress under compression than in tension. This reduced the load bearing resistance by approximately 30%. It is recommended to investigate glass-steel columns with higher steel yield stress under compression than used in the present research project.
4. It is recommended to further fine tune the FE model based on additional data from more experiments. Then, a parameter study to investigate the effect of salient parameters on the failure behaviour of the glass-steel column can be carried out.

## References

- [1] Overend, M. (2005), The Design, Assembly & Performance of Glass Columns, *Glass processing days 2005*, New Product Developments and Applications, pp. 1-5
- [2] Nieuwenhuijzen, E.J. van (2005), The Laminated Glass Column, *Glass processing days 2005*, Building Projects Case Studies, pp. 1-4
- [3] Luible, A. (2004), *Stabilität von Tragelementen aus Glas*, PhD thesis, EPFL, Thèse no 3014, Lausanne, Switzerland
- [4] Roebroek, F.J.A. (2009), Design of a Transparent Column in Glass and Steel, research report number ARR 2009 BWK 4578, master thesis, Dept. of the Built Environment, Eindhoven University of Technology, Eindhoven, The Netherlands
- [5] Roebroek, F.; Snijder, H.H.; Herwijnen, F. van; Huveners, E.M.P. (2010), Design of a transparent column in glass and steel, *Challenging Glass 2 – Conference on Architectural and Structural Applications of Glass*, Bos – Louter - Veer (Eds.), Delft University of Technology, pp. 1-10
- [6] Dierks, D. (2012), A Slender High Strength Steel Column Laterally Supported by Glass Panes, research report number A-2012.21/O-2012.21, master thesis, Dept. of the Built Environment, Eindhoven University of Technology, Eindhoven, The Netherlands
- [7] *NEN-EN-1993-1* (2006), Eurocode 3: Design of steel structures - Part 1-1: General rules and rules for buildings
- [8] Bos, F.P. (2009), *Safety Concepts in Structural Glass Engineering*, PhD Thesis, Delft University of Technology, Delft, The Netherlands
- [9] European Technical Approval DYWIDAG Spannsysteme, ETA-05/0123, Dywidag product data sheet
- [10] Johansson, B.; Collin, P. (2005), Eurocode For High Strength Steel and Applications in Construction, 1st International Conference on Super-High Strength Steels, 2 - 4 November 2005, Rome, Italy, Publisher Associazione Italiana di Metallurgia, Milano, 12 pp.
- [11] 3M Scotch-Weld 9323 B/A (1996), Structural Adhesive, Product Data Sheet
- [12] Huveners, E.M.P. (2009), *Circumferentially Adhesive Bonded Glass Panes for Bracing Steel Frames in Façades*, PhD Thesis, Eindhoven University of Technology, Eindhoven, the Netherlands
- [13] *NEN-EN-10002-1* (2001), Metallic materials - Tensile testing - Part 1: Method of test at ambient temperature

[14]Ziemian, R.D. (2010), *Guide to Stability Design Criteria for Metal Structures*, John Wiley & Sons

[15]ANSYS *structural analysis guide*, release 11.0, ANSYS Inc (2009)